Biochimica et Biophysica Acta, 688 (1982) 764–774
Elsevier Biomedical Press

BBA 71232

RESOLUTION OF PLASMA MEMBRANE LIPID FLUIDITY IN INTACT CELLS LABELLED WITH DIPHENYLHEXATRIENE

D. GRUNBERGER, R. HAIMOVITZ and M. SHINITZKY *

Department of Membrane Research, The Weizmann Institute of Science, Rehovot (Israel)

(Received October 30th, 1981)

Key words: Membrane fluidity; Fluorescence labeling

The partitioning of fluorescence probes into intracellular organelles poses a major problem when fluorescence methods are applied to evaluate the fluidity properties of cell plasma membranes with intact cells. This work describes a method for resolution of fluidity parameters of the plasma membrane in intact cells labelled with the fluorescence polarization probe 1,6-diphenyl-1,3,5-hexatriene (DPH). The method is based on selective quenching, by nonradiative energy transfer, of the fluorescence emitted from the plasma membrane after tagging the cell with a suitable membrane impermeable electron acceptor. Such selective quenching is obtained by chemical binding of 2,4,6-trinitrobenzene sulfonate (TNBS), or by incorporation of *N*-bixinoyl glucosamine (BGA) to DPH-labelled cells. The procedures for determination of lipid fluidity in plasma membranes of intact cells by this method are simple and straightforward.

Introduction

The lipid fluidity of the cell plasma membrane is implicated in many cellular processes such as transformation [1,2], mitogenesis [3,4], cell cycling [5,6], differentiation [7–10] and proliferation [11–13], and can be regarded as fundamental regulator of cellular function [14]. The fluorescence polarization with DPH as a probe is now widely used as a simple and reproducible technique for evaluation of average lipid fluidity parameters in membranes [15]. Unfortunately, labelling of intact cells with DPH, as well as with most other probes, is followed by a progressive incorporation of the probe into intracellular organelles and the apparent fluidity values are in fact a weight average of all labelled lipid domains [15–17]. Yet, in situ measurements of plasma membrane properties are advantageous over membrane fractionation, since it is likely that during the process of isolation, selective membrane domains may be detached, which may lead to erroneous fluidity values. Direct in situ measurements are in principle possible, by selective tagging of the cell plasma membrane with an efficient impermeable fluorescence quencher. This approach and its related techniques are described in this article.

Materials and Methods

Reagents

Colour-free 2,4,6-trinitrobenzenesulfonic acid (TNBS) was purchased from Eastman Kodak. Neutralization of TNBS was carried out by adding an equivalent amount of solid sodium bicarbonate to TNBS in 1 ml chloroform, drying under nitrogen and resuspending in phosphate-buffered saline pH 7.2. This procedure was found to avoid chemical decomposition which is displayed by a yellow

* To whom correspondence should be addressed.

Abbreviations: DPH, 1,6-diphenyl-1,3,5-hexatriene; TNBS, 2,4,6-trinitrobenzene sulfonate; BGA, *N*-bixinoylglucosamine.

0005-2736/82/0000–0000/$02.75 © 1982 Elsevier Biomedical Press

colouring of the solution when neutralization is carried out in water.

Picryl chloride (Fluka) was introduced into phosphate-buffered saline by a 1:100 dilution of ethanolic solution.

Dispersion of $2 \cdot 10^{-6}$ M DPH (Koch-Light) was prepared by 1:1000 dilution of a stock solution of $2 \cdot 10^{-3}$ M in tetrahydrofuran into vigorously stirred phosphate-buffered saline [3,13].

Preparation of BGA was carried out as follows. Bixin (from Kasei, Tokyo), a natural highly coloured carotenoid fatty acid [18], was first mixed in ethyl acetate (1 g/50 ml) at room temperature for 10 min and the undissolved impurities (approx. 30%) were separated and discarded. The concentration of bixin (or its derivatives) was estimated spectrophotometrically using $\epsilon_{475} = 125000$ $M^{-1} \cdot cm^{-1}$ [18]. The active *N*-hydroxysuccinimide ester of bixin was prepared by adding 20% excess of *N*,*N'*-dicyclodexylcardiondiimide (DCC, Fluka) and equimolar *N*-hydroxysuccinimide. The mixture was stirred in the dark under argon at room temperature for 8 h and then supplemented with 1-hydroxybenzotriazole (Sigma) to afford maximum esterification. Thin-layer chromatography (chloroform/methanol/water, 65:25:4) indicated about 80% conversion to the active ester. The precipitated material was removed, the solution was evaporated to complete dryness and taken up in dimethylformamide and a desired portion was diluted in 1:1 dimethylformamide/water mixture (solution 1). An aqueous solution of glucosamine hydrochloride was brought to pH 9 with sodium carbonate and then diluted 1:1 with dimethylformamide (solution 2). Solutions 1 and 2 were mixed so that glucosamine was at a 3–5-fold molar excess and the reaction mixture was left at room temperature in the dark under argon for several days, this being followed by thin-layer chromatography (as above), which indicated three major products. The products were isolated by preparative thin-layer chromatography and analysed for optical activity. Only one product displayed such an activity ($R_F = 0.57$) and was taken to be the BGA, which was confirmed by nitrogen analysis. BGA was kept under argon in the dark at −20°C as $4 \cdot 10^{-5}$ M solution in tetrahydrofuran.

Membranes

Leaky human erythrocyte membranes were prepared by the method of Dodge et al. [19]. Synaptosomes from rat brain were prepared according to Hershkowitz [20] and sealed sarcoplasmic reticulum from rabbit muscle as described by Meissner [21]. Sealed chromaffin granules from bovine adrenal glands [22] and Sindbis virus [23] were prepared as described. The plasma membrane of mice spleen cells and EL-4 lymphoma cells (see below) were isolated essentially as described by Gotlib [24,25].

Cells

Normal and transformed cells were examined. Spleen cells and thymocytes were isolated from Balb/c mice. Macrophage exudates were from Balb/c peritoneum cavity after thioglycollate treatment [26]. EL-4 lymphoma cells were maintained as ascites tumour in the peritoneum cavity of syngeneic C57b1 mice. Cultured Balb/c fibroblasts in suspension were from the 3T3 line. Friend erythroleukemic cells (strain No. 745) were harvested at confluency.

Murine L cells from strain No. 929 were grown as a cultured monolayer in Eagle's medium (Gibco F-16), supplemented with 8% calf serum, 2.25 mg/ml sodium bicarbonate, 3.5 mg/ml glucose and 2.95 mg/ml Difco tryptose phosphate broth. Inclusion of neutral lipids into the cytoplasm of these cells was carried out by a method described for LM cells [27]. Accordingly, 40 μg/ml ethanolamine were added to the incubation serum-medium and the cells were incubated for 80 h (5% CO_2) and subsequently washed in medium only. The cells were removed, suspended in 10 ml medium, washed twice in phosphate-buffered saline and resuspended to a final conentration of $2 \cdot 10^6$ cells/ml.

Labelling of membranes

A series of samples of 50 μl packed membranes in 2.5 ml phosphate-buffered saline were mixed with 2.5 ml DPH dispersion in 15 ml Sorvall test tubes. Samples were incubated (30 min, 37°C, mildly shaking bath) and subsequently centrifuged (15 min, 4°C, 15000 rpm). Supernatants were dis-

carded. The DPH-labelled packed membranes were resuspended to a final volume of 1 ml to which increasing amounts of TNBS were added from a stock solution of 3.5 mg/ml TNBS ($1 \cdot 10^{-2}$ M) in phosphate-buffered saline. The reaction proceeded for 1 h at 4°C and was terminated by addition of 9 ml cold phosphate-buffered saline followed by immediate centrifugation as described above. Supernatants were discarded and samples were resuspended in 5 ml phosphate-buffered saline. Quenching of DPH fluorescence in isolated membranes by BGA was carried by dilution of its tetrahydrofuran solution ($4 \cdot 10^{-5}$ M) 100–1000-fold into the DPH-labelled membranes. Incorporation of BGA was monitored by fluorescence quenching.

Labelling of cells

Suspensions of $4 \cdot 10^6$–$1 \cdot 10^7$ cells in 5 ml phosphate-buffered saline were mixed with 5 ml DPH dispersion. After 30 min incubation at 37°C each sample was divided equally into two groups and spun down (1200 rpm, 5 min). One sample, which served as a control, was resuspended in 1 ml cold phosphate-buffered saline and the other was treated with 1 ml TNBS solution (2 mg/ml). The reaction was carried out for 1 h at 4°C, terminated by dilution and centrifugation as described above. Supernatants were discarded and samples were resuspended to a final volume of 2–5 ml phosphate-buffered saline. Viability, checked by Trypan blue exclusion, was above 90% in all TNBS-treated cells.

A second labelling method consisted of reacting four or five separate samples of $2 \cdot 10^6$–$5 \cdot 10^6$ DPH-labelled cells with 1 ml phosphate-buffered saline containing increasing concentrations of TNBS (0–1 mg/ml). The first of the samples served as a control and was resuspended in 1 ml cold phosphate-buffered saline. The rest of the procedure was identical to the labelling method described above. BGA incorporation was carried out as for isolated membranes (see above).

Fluorescence measurements

Fluorescence intensity (F) and polarization were measured with a fluorescence polarization instrument as previously described [1]. F was normalized according to protein content in isolated membranes and number of cells in each cell sample. Microviscosity was estimated from fluorescence polarization as described [15].

Results and Discussion

The absorption spectrum of the yellow product trinitrophenyl-modified lysine residues, obtained by reacting TNBS with proteins, and the blue fluorescence spectrum of DPH, have an overlap region which can mediate the quenching of the latter by nonradiative energy transfer [28]. A model compound for TNBS conjugated to proteins was prepared by reacting TNBS with poly(L-lysine), the absorption of which is shown in Fig. 1. The figure also displays the emission spectrum of DPH in hexane as a model for fluorescently labelled membranes. As clearly demonstrated, there is a substantial overlap between the two spectra. The analogous spectra for DPH and BGA are given in Fig. 2.

The efficiency of quenching by nonradiative energy transfer is characterized by the distance, R_0, between donor and acceptor molecules at which 50% of the fluorescence is quenched. This value can be calculated according to the well-known Förster equation [28]:

$$R_0^6 = \frac{9000(\ln 10)\kappa^2}{128\pi^5 n^4 N} q \int_0^\infty f\mathrm{A}^*(\lambda) \cdot \epsilon_\mathrm{B}(\lambda) \cdot \lambda^4 \, \mathrm{d}\lambda \quad (1)$$

where q is the fluorescence quantum yield of the

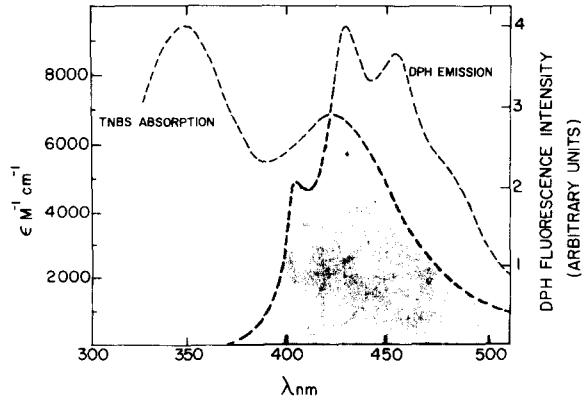

Fig. 1. Absorption spectrum of TNBS conjugated to poly(L-lysine) in phosphate-buffered saline and emission spectrum of DPH in hexane ($\lambda_{ex} = 353$ nm).

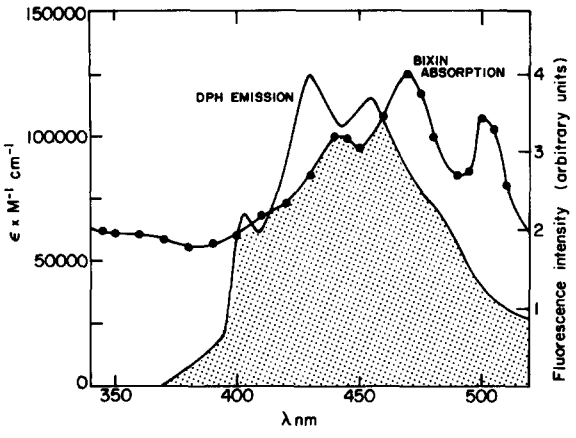

Fig. 2. Absorption spectrum of BGA in ethanol (●——●) and emission spectrum of DPH in hexane.

donor A* in the absence of acceptor molecules, n is the refractive reflex of the medium, N is Avogado's number, $fA^*(\lambda)$ is the normalized fluorescence intensity of A* at wavelength λ, $\epsilon_B(\lambda)$ is the extinction coefficient of the acceptor B at λ, and κ is an orientation factor. In systems which undergo rapid rotatory Brownian motion during the lifetime of the excited state $\kappa^2 = 2/3$. The integral in Eqn. 1, (J), represents the normalised overlap between donor emission and acceptor absorption and is the main variable in this equation.

Assuming that Eqn. 1 is also valid for the DPH-TNBS couple in biological membranes, insertion of numerical values for the constants appearing in Eqn. 1 leads to [29]:

$$R_0(\text{Å}) = 9.79 \cdot 10^3 \left(\kappa^2 q J n^{-4}\right)^{1/6} \qquad (2)$$

From measured data of Fig. 1 we have calculated $J = 1.65 \cdot 10^{-14}$ cm^6/mmol. The other values were taken as $n = 1.4$ and $q = 0.8$ [30], leading to $R_0 \approx 35$ Å between DPH and TNP residues. This value is still within effective distance limitations of membrane bilayers. Analogously, Eqn. 1 and the overlap integral evaluated from Fig. 2, yielded $R_0 \approx 60$ Å for energy transfer from DPH to BGA.

Membranes

Unsealed brain synaptosomes and erythrocyte ghosts, as well as sealed sacroplasmic reticulum, were used in order to define the conditions for maximum quenching of the DPH fluorescence by TNBS labelling. Results, which are displayed in Fig. 3, indicate that in these membranes over 90% quenching of the fluorescence intensity is achieved by 1 h incubation at 4°C with 1 mg/ml TNBS (see Table I). Changing pH between 7 and 8 produced no significant deviation in quenching efficiency. The contribution to quenching by radiative energy transfer, namely light emitted by DPH which is then absorbed by TNBS (inner filter effect), was assumed to be negligible. This mechanism is effective only at local quencher concentrations above $A = 0.1$. It was estimated that the inner filter of TNBS in the labelled membranes had an absorbance which was at least one order of magnitude lower.

The number of trinitrophenyl-modified residues bound to these membranes at approx. 90% quenching was estimated by solubilizing the membranes in 0.1 M NaOH, which was accompanied by substantial spectral changes as demonstrated in Fig. 4. An extinction coefficient at 410 nm of $\epsilon = 15000$ cm$^{-1} \cdot$ M^{-1} was estimated for the trinitrophenyl-protein conjugate in 0.1 M NaOH. The protein content of the membrane samples was quantified [31], and the number of trinitrophenyl

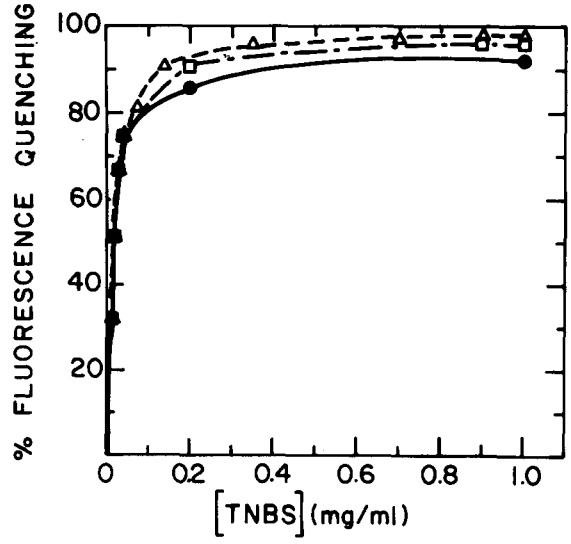

Fig. 3. Fluorescence quenching of DPH in sarcoplasmic reticulum (●——●); erythrocyte ghosts (△——△); and brain synaptosomes (□——□), at different concentrations of TNBS. Incubation was carried out for 1 h at 4°C in phosphate-buffered saline.

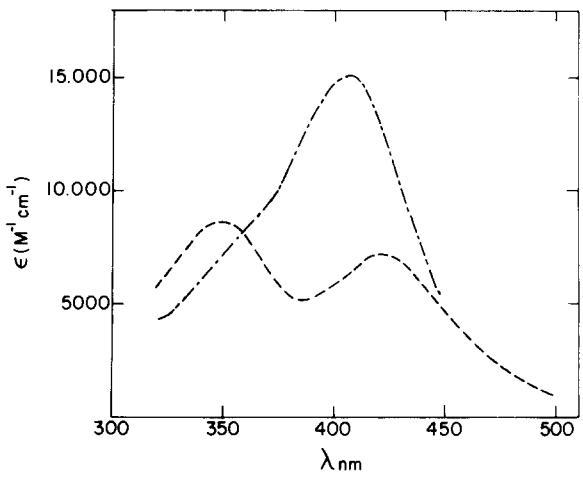

Fig. 4. Absorption spectrum of TNBS conjugated to poly(L-lysine) in phosphate-buffered saline (------) and in 0.1 M NaOH (·–·–·).

moieties was correlated with the number of amino acids assuming an average molecular weight of 120. In all three membranes 90% quenching corresponded to one trinitrophenyl residue per 100–150 amino acid residues.

The quenching efficacy of BGA was similarly tested with unsealed human erythrocyte membranes. Packed DPH-labelled membranes (see Materials and Methods) were diluted 1:100 with phosphate-buffered saline and their fluorescence intensity and polarization were recorded. BGA was then added from tetrahydrofuran solution ($4 \cdot 10^{-5}$ M) to form a final solution in the range of $4 \cdot 10^{-7}$–$4 \cdot 10^{-8}$ M ($A_{max} < 0.05$). A progressive decrease in fluorescence intensity took place immediately upon addition of BGA. At concentrations above $1 \cdot 10^{-7}$ M BGA the quenching of DPH fluorescence reached 90% after less than 5 min. The fluorescence quenching is presumably a direct result of BGA partitioning, and if one assumes practical complete incorporation, the number of BGA molecules in the membrane in these experiments is in the order of 1/100 to 1/1000 per membrane lipid. A similar range of concentration also applies for DPH in the membrane, and even at these high dilutions the energy transfer is still effective because of the high R_0 value.

In a true isotropic solution of quencher and fluorophore, reduction in fluorescence intensity (F) by quenching is accompanied by an equivalent reduction in the average excited state lifetime, τ, of the fluorophore. The reduction in τ will further increase the apparent fluorescence anisotropy (r) according to the Perrin equation:

$$r_0/r = 1 + \frac{3\tau}{\rho} \tag{3}$$

where r_0 is the experimental upper limit of fluorescence anisotropy and ρ is the rotational relaxation time of the fluorophore. Thus, the dependence of r on F in an isotropic solution can be described by:

$$F \propto r_0/r - 1 \tag{4}$$

The increase in fluorescence anisotropy of DPH which followed TNBS quenching was much lower than that expected from Eqn. 4. As an example, Fig. 5 describes the measured r values at different F levels obtained by increasing TNBS concentration in brain synaptosomes. The expected increase in r with decrease of F, evaluated according to Eqn. 4, is also described in this figure. As shown, the measured r reaches a plateau level which is much lower than the expected value of $r_0 = 0.362$ which is approached in the theoretical curve. This

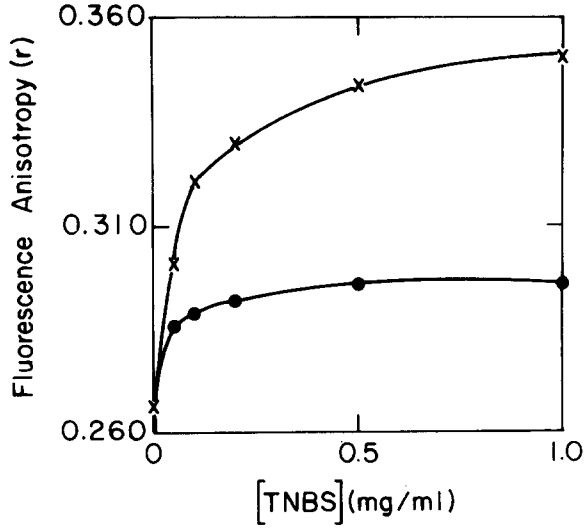

Fig. 5. Fluorescence anisotropy of DPH-labelled brain synaptosomes after 1 h reaction at different concentrations of TNBS at 4°C (●———●). The theoretical fluorescence anisotropy estimated from Eqn. 4 is also shown (×———×).

inconsistency presumably originates from the quencher-fluorophore organization in the labelled membrane which is non-isotropic. The experimental curve is compatible with a selected population of DPH molecules which is practically fully quenched and a second population which is virtually unavailable for quenching. The proportions of these two sub-populations presumably change with increase of bound trinitrophenyl-modified residues.

The increase in fluorescence polarization by fluorescence quenching with BGA was much smaller than with TNBS (data not shown). The reason for this is as yet unclear.

In unsealed membranes, unlike whole cells, TNBS can bind to both sides of the bilayer. Therefore, the saturation of TNBS-binding sites on cell surfaces may result in only partial quenching of the plasma membrane fluorescence. To evaluate the effectiveness of such one-sided labelling, sealed vesicles from different sources were reacted with TNBS at a concentration of 2 mg/ml, which in unsealed membranes resulted in over 90% quenching (see Fig. 3). Labelling was also carried out after brief sonication (10 s) to provide samples labelled on both sides of the membrane. The results, given in Table I, indicate that selective labelling of one side of the membrane with TNBS may only partially quench DPH fluorescence. Since TNBS can bind to both proteins and phospholipids (i.e., phosphatidylethanolamine and phosphatidylserine) their density and distribution in the outer membrane leaflet would determine the capacity of quenching in sealed structures.

TABLE I

MAXIMUM QUENCHING OF DPH FLUORESCENCE BY TNBS LABELLING IN SEALED AND DISRUPTED MEMBRANES

Membrane	Percent quenching (sealed)	Percent quenching (sonicated)
Human erythrocytes	25–50	98
Sindbis virus	57	–
Chromaffin granules	87	95
Sarcoplasmic reticulum	92	98

Intact cells

TNBS has been used as a membrane impermeable reagent in many studies [32–35]. However, recent works have shown that under certain conditions TNBS can penetrate through the membrane and label inner components [36–38]. To verify whether under our experimental conditions (1 h, 4°C, 2 mg/ml) such penetration occurs, cells were labelled with increasing concentrations of TNBS, and its permeable analogue picryl chloride. Quenching of fluorescence intensity in the intact cells was compared with quenching of the fluorescence signal in sonicated cell samples. Results using EL-4 ascites tumor cells, as a model cell system, are shown in Fig. 6. They indicate that similarly to DPH quenching in membranes, the maximum fluorescence quenching is achieved by 1 h incubation with 2 mg/ml TNBS at 4°C. The residual fluorescence presumably originates from DPH-labelled intracellular organelles and from unquenched plasma membrane regions. The plateau level of quenching (Fig. 6) is maintained for up to 1.5 h of treatment, after which there is a slow but consistent decrease in fluorescence inten-

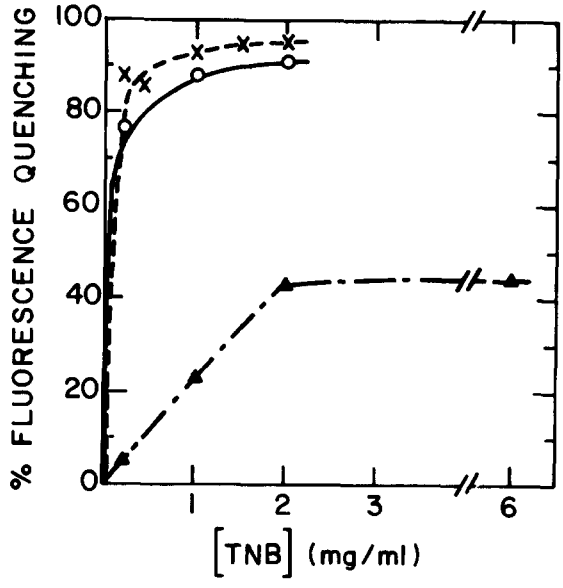

Fig. 6. Fluorescence quenching in DPH-labelled EL-4 lymphoma cells ($2 \cdot 10^6$ cells/ml) with increasing amounts of TNBS (▲——▲), TNBS after sonication (×——×), and picryl chloride (○——○). Reaction was carried out in phosphate-buffered saline for 1 h at 4°C.

sity reflecting slow penetration of TNBS into the cell.

Both labelling with picryl chloride and sonication with TNBS resulted in loss of at least 90% fluorescence intensity at relatively low concentrations of reactant.

Fatty acid acyl derivatives of glucosamine partition readily into biological membranes, similarly to the free acid, but are not transported intracellularly because of the membrane-impermeable glucosamine residue [39]. It was therefore reasoned that when taken up by cells, BGA should incorporate exclusively into the cell plasma membranes, while underivatized bixin will eventually partition into all lipid domains in the cell. To verify this assumption, the fluorescence intensities of DPH-labelled mouse splenocytes and EL-4 cells ((2–4) · 10^6 cells/ml in phosphate-buffered saline) were measured after addition of $1 \cdot 10^{-7}$ M BGA (see above) or $1 \cdot 10^{-7}$ M bixin. While with bixin the fluorescence decreased with time almost to the background level, indicating practically full quenching of DPH fluorescence, the fluorescence quenching with BGA levelled off in both cells at a particular intensity. Further addition of $1 \cdot 10^{-7}$ M BGA reduced the fluorescence intensity by only an insignificant amount. Typical fluorescence quenching profiles with bixin and BGA are shown in Fig. 7. The remaining approx. 60% fluoresence intensity after exhaustive quenching with BGA presumably originates from the intracellular organelles.

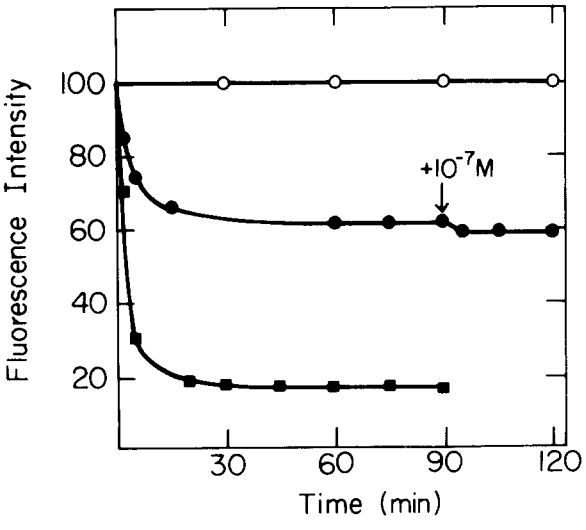

Fig. 7. Fluorescence quenching of DPH-labelled mouse splenocytes ($2 \cdot 10^6$/ml) in PBS (○——○) upon the addition of $1 \cdot 10^{-7}$ M bixin (■——■) and $1 \cdot 10^{-7}$ M BGA (●-●). A second addition of $1 \cdot 10^{-7}$ M BGA is marked.

Based on the above findings, two procedures for evaluation of plasma membrane fluidity with intact cells were developed. In the first method it is assumed that tagging with TNBS or BGA results in complete and selective quenching of the DPH fluorescence emitted from the cell plasma membrane. Since complete quenching of DPH is sealed vesicles is not always achieved, this method should be considered as semi-quantitative. DPH-labelled cells ((2–5) · 10^6/ml) were divided into two equal groups, one was treated with 2 mg/ml TNBS for 1 h at 4°C and the other with phosphate-buffered saline (control). The fluorescence intensity (F) and anisotropy (r) were measured simultaneously. If one assumes that the system is composed of a series of fluorescing compartments of different accessibility to TNBS then [40]:

$$r = \Sigma f_i r_i \tag{5}$$

where f_i is the fraction of fluorescence intensity of compartment i. Reducing Eqn. 5 to a binary system composed of the plasma membrane and the intracellular organelles leads to:

$$r = \frac{F_{in}}{F} r_{in} + \frac{F - F_{in}}{F} r_m \tag{6}$$

where r and F are the apparent anisotropy and fluorescence intensity values of the control sample, r_{in} are the measured values in the TNBS-prelabelled cells and r_m is the plasma membrane anisotropy value. Thus, by assuming complete and selective quenching, the fluidity properties of the cell plasma membranes can be determined by simple rearrangement of Eqn. 6:

$$r_m = \frac{\left[r - \frac{F_{in}}{F} r_{in}\right] F}{F - F_{in}} \tag{7}$$

Analogous procedure applies also to BGA, where DPH-labelled cells are divided into two equal

groups; one is left untreated and the other is treated with $2 \cdot 10^{-7}$ M BGA for 20 min. Evaluation of r_m is carried out as with TNBS treatment. Table II summarizes the measured fluidity parameters of membranes of various cell types and their corresponding microviscosity ($\bar{\eta}$) values obtained by the above method with TNBS. The table also includes the apparent r and $\bar{\eta}$ values for the same cells without TNBS treatment.

The second method takes into consideration the fact that in whole cells complete quenching of the surface membrane fluorescence may not always be possible and the following alternative is therefore suggested. Four of five cell samples labelled with DPH are allowed to reach various levels of fluorescence quenching by reaction with increasing concentrations of TNBS (0–1 mg/ml), and the r and F values of each sample are subsequently measured. Since with isolated membranes, TNBS quenching did not affect the apparent r value much (see Fig. 3), one can assume that in TNBS-labelled cells the residual r_m remains constant. Eqn. 6 can therefore be rearranged to the convenient form

$$r = \frac{F_{in} r_{in} - F_{in} r_m}{F} + r_m = \text{const.} \cdot \frac{1}{F} + r_m \qquad (8)$$

where r_{in} and r_m are constants. By plotting the measured r values against $1/F$, r_m could be obtained by extrapolation of the straight line to $1/F = 0$. Fig. 8 represents a plot of r vs. $1/F$

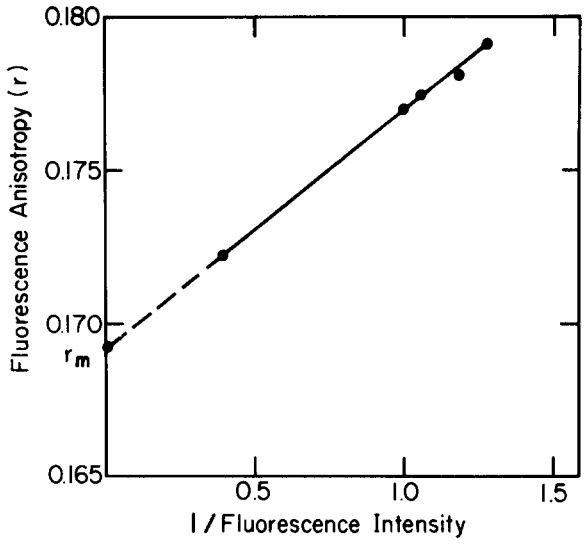

Fig. 8. The dependence of fluorescence anisotropy on the reciprocal of fluorescence intensity in DPH-labelled EL-4 lymphoma cells quenched to different levels by TNBS tagging.

obtained with DPH-labelled EL-4 cells stained to different degrees with TNBS. The r_m (25°C) value obtained was 0.169, which corresponds to $\bar{\eta} \approx 2.1$ P. The first method yielded r_m (25°C) = 0.163 and $\bar{\eta} \approx 1.9$ P, while direct measurements with intact cells without TNBS quenching yielded an apparent r (25°C) = 0.177 and $\bar{\eta} \approx 2.3$ P.

The second method with BGA is considerably simpler. The fluorescence intensity and polarization of DPH-labelled cells ($(2–5) \cdot 10^6$/ml) is first

TABLE II

APPARENT FLUIDITY PROPERTIES OBTAINED WITH DPH-LABELLED CELLS BEFORE AND AFTER FLUORESCENCE QUENCHING WITH TNBS

Cell	Maximum fluorescence quenching (%) [a]	Total		Residual		Plasma membrane	
		r (25°C)	$\bar{\eta} \pm 15\%$ (poise)	r_{in}	$\bar{\eta} \pm 15\%$ (poise)	r_m	$\bar{\eta} \pm 15\%$ (poise)
Balb/c thymocytes	30	0.200	2.96	0.201	3.00	0.198	2.90
Balb/c splenocytes	35	0.185	2.47	0.174	2.18	0.207	3.23
Friend erythroleukemia	32	0.235	4.44	0.263	6.37	0.176	2.27
Differentiated Friend leukemia	11	0.214	3.47	0.215	3.51	0.206	3.17
3T3 fibroblasts	33	0.196	2.83	0.196	2.83	0.196	2.83
Murine macrophages	48	0.223	3.85	0.223	3.85	0.223	3.85
EL-4 lymphoma	44	0.177	2.30	0.189	2.62	0.163	1.90

[a] In all cases over 90% quenching was obtained after brief sonication when internal membranes became available for TNBS labelling.

recorded and then $2 \cdot 10^{-7}$ M BGA is added. F and r recorded at time intervals till no more fluorescence quenching is observed (approx, 20 min) and plotted according to Eqn. 8. Table III summarises results of cell plasma membranes obtained by the second method with TNBS and BGA. Analogous results obtained with isolated plasma membranes are also presented.

The second labelling method was further verified in L cells grown on medium containing ethanolamine (see Materials and Methods), which presumably increases the intracellular neutral lipid level [27]. The results presented in Fig. 9 clearly demonstrate that the intracellular microviscosity in the cells grown with ethanolamine is substantially lower than that of the plasma membrane, in agreement with published data [27]. In contrast, the control cells exhibit a higher intracellular microviscosity. The extrapolated values of r_m are very similar for both cells, with a small increment of fluidisation in the ethanolamine-treated cells which may reflect minor inclusions of neutral lipids into the plasma membrane.

The extrapolated value of r_m is formally attributed to the quenchable region of the DPH-labelled cells which is ascribed to the cell plasma membrane. To a first approximation, r_m can represent the mean lipid fluidity of the cell plasma membranes, since the apparent r of isolated membranes is affected only slightly by the degree of fluorescence quenching (Fig. 5). This indicates that, even through the fluorescence quenching at the plasma membrane is only partial, it is appoximately evenly distributed over the various lipid compartments. The value for r_{in}, is a combination of the unquenchable DPH-labelled regions,

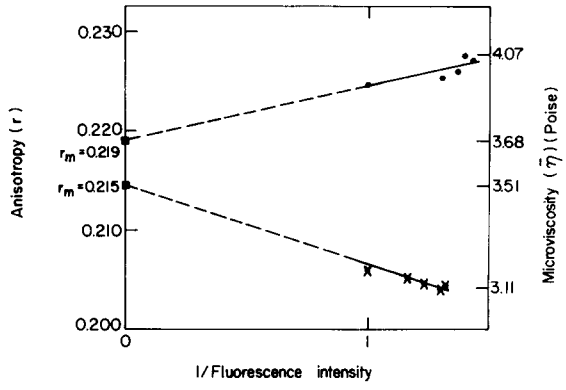

Fig. 9. The dependence of fluorescence anisotropy on the reciprocal of fluorescence intensity in DPH-labelled L cells quenched to different levels by TNBS tagging in control cells (O——O) and cells grown in the presence of ethanolamine (×——×).

which consist mostly of intracellular compartments with some contribution from the unquenched region of the plasma membrane (see Table I). Therefore, when the second method is employed for evaluation of r_{in}, the contribution of the unquenchable fluorescence of the plasma membrane should be taken into account.

In some of the cell types investigated (see Table II), there is an unexpected similarity between r_m and r_{in}. In macrophages this feature may result from phagocytic activity which enriches the cytoplasm with plasma-membrane fragments. The regeneration of the plasma membrane, which compensates for membrane internalization, operates by both biosynthetic and recycling processes. The latter process was proposed for the membrane

TABLE III

RESOLVED VALUES OF DPH FLUORESCENCE ANISOTROPY (r_m) AND THE CORRESPONDING MICROVISCOSITY OF CELL PLASMA MEMBRANES OBTAINED ACCORDING TO Eqn. 8 BY QUENCHING WITH TNBS AND BGA

Values obtained with isolated membranes are also presented for comparison.

	TNBS quenching		BGA quenching		Isolated membranes	
	r_m (25°C)	$\eta \pm 15\%$	r_m (25°C)	$\eta \pm 15\%$	r (25°C)	$\eta \pm 15\%$
Mouse splenocytes	0.210	3.26	0.220	3.64	0.230	4.18
EL-4 lymphoma	0.169	2.10	0.165	2.02	0.164	1.98

lipids [41] through a mechanism of continuous lipid flow between the external and internal cellular membranes [42]. Among the cells investigated, the transformed cells (i.e., EL-4 lymphoma, Friend erythroleukemic and L cells) display a distinct fluidity difference between the plasma membrane and inner membrane compartments. Since these cells proliferate continuously, it is reasonable to assume that the rate of proliferation overrides processes of fluidity equilization between the inner and outer cellular domains.

Methodological remarks

Lipid fluidity derived by fluorescence depolarization can be expressed at different levels of quantitivity. On a relative semiquantitative scale, the lipid microviscosity $\bar{\eta}$ can be presented in units of $(r_0/r-1)^{-1}$ (see Eqn. 3), which can be converted to macroscopic units (i.e., poise) upon multiplication by an empirical factor [15]. More quantitative $\bar{\eta}$ values can be derived from calibration curves of proper fluids [15,43,44]. The translation of the apparent diffusion of the probe in the membrane to macroscopic viscosity has been recently seriously challenged by the finding that in many membranes time-resolved fluorescence anisotropy of DPH does not decay to zero, as expected for unrestricted rotation, but approaches a finite nonzero r_∞ value (for summary see Refs, 45, 46). This is undoubtedly due to preferential alignment of DPH along the lipid chains [47], which increases (r_∞ increases) as the apparent viscosity (higher r) increases [45].

Therefore the apparent value of $\bar{\eta}$ obtained by the macroscopic simulation is actually a combination of the degree of order in the system (presented by the 'order parameter' r_∞/r_0 (Refs 45, 48) and the 'true' microviscosity $\bar{\eta}_0$. The empirical correlation between the 'true' and the apparent microviscosities is approximately given by [46]:

$$\bar{\eta}_0 = \left(\frac{0.089}{r} - 0.116\right)\bar{\eta} \qquad (9)$$

and indicates that the true microviscosity is considerably smaller than the apparent microviscosity. These recent developments enable the evaluation of the true microviscosity, as well as the degree of order in lipid layers by the simple steady-state fluorescence depolarization method. These parameters, in addition to the apparent $\bar{\eta}$, provide a comprehensive view on the lipid dynamics. With the aid of the methods described in this paper, such an analysis can now be extended to cell plasma membranes in intact viable cells.

Finally, the results of lipid dynamics obtained by the fluorescence polarization methods are of low microscopic resolution and can be classified as 'submacroscopic' [46]. However, this submacroscopic presentation of lipid dynamics is of direct physiological relevance and is of great importance when a membranal function is correlated with the lipid fluidity [49].

Acknowledgement

This investigation was supported by Grant Number 5 RO1 CA 27471-03, awarded by the National Cancer Institute, U.S. Department of Health, Education and Welfare.

References

1 Shinitzky, M. and Inbar, M. (1974) J. Mol. Biol. 85, 603–615
2 Hilgers, J., Van der Sluis, P.J., Van Blitterswijk, W.J. and Emmelot, P. (1978) Brit. J. Cancer 37, 329–336
3 Inbar, M. and Shinitzky, M. (1975) Eur. J. Immunol. 5, 116–170
4 Ferber, E., de Pasquale, G.G. and Resch, K. (1975) Biochim. Biophys. Acta 398, 364–376
5 De Laat, S.W., Van der Saag, P.T. and Shinitzky, M. (1977) Proc. Natl. Acad. Sci. U.S.A. 74, 4458–4461
6 De Laat, S.W., Van der Saag, P.T., Elson, E. and Schlessinger, J. (1980) Proc. Natl. Acad. Sci. U.S.A. 77, 1526–1528
7 Arndt-Jovin, D.J., Ostertag, W., Eisen, H., Klimek, F. and Jovin, T.M. (1976) J. Histochem. Cytol. 24, 332–342
8 Kawasaki, Y., Wakayama, N., Koike, T., Kawai, M. and Amano, T. (1978) Biochim. Biophys. Acta 509, 440–449
9 De Laat, S.W., Van der Saag, P.T., Nelemans, S.A. and Shinitzky, M. (1978) Biochim. Biophys. Acta 509, 188–193
10 Ip, S.H.E. and Cooper, R.A. (1980) Blood 56, 227–232
11 Inbar, M., Yuli, I. and Raz, A. (1977) Exp. Cell Res. 105, 325–335
12 Cheng, S. and Levy, D. (1979) Arch. Biochem. Biophys. 196, 424–429
13 Muller, C.P., Wolloch, Z. and Shinitzky, M. (1980) Cell Biophys. 2, 233–240
14 Shinitzky, M. and Henkart, P. (1979) Int. Rev. Cytol. 60, 121–147
15 Shinitzky, M. and Barenholtz, Y. (1978) Biochim. Biophys. Acta 515, 367–394

16 Berlin, R.D. and Ferg, J.P. (1977) Proc. Natl. Acad. Sci. U.S.A. 74, 1072–1076
17 Johnson, S.M. and Nicolau, C. (1977) Biochem. Biophys. Res. Commun. 76, 869–874
18 Zechmeister, A. (1960) Fortschr. Chem. Org. Naturst. 18, 320–333
19 Dodge, J.T., Mitchell, C.M., Hanahan, D.J. (1963) Arch. Biochem. Biophys. 100, 119–130
20 Hershkowitz, M. (1978) Biochim. Biophys. Acta 542, 274–283
21 Meissner, G. (1974) Methods Enzymol. 31, 238–246
22 Trifano, J.M. and Dworkind, J. (1970) Anal. Biochem. 34, 403–412
23 Pfeffercorn, E.R. and Hunter, H.S. (1963) Virology 20, 433–435
24 Gotlib, L.J. and Searls, D. (1980) Biochim. Biophys. Acta 602, 207–212
25 Gotlib, L.J. (1982) Biochim. Biophys. Acta 685, 21–26
26 Bar-Shavit, Z., Stabinsky, Y., Fridkin, M. and Goldman, R. (1979) J. Cell. Physiol. 100, 55–62
27 Esko, J.D., Gilmore, J.R. and Glaser, M. (1977) Biochemistry 16, 1881–1890
28 Förster, J. (1948) Ann. Physik. 2, 55–75
29 Stryer, L. and Haugland, R.P. (1967) Proc. Natl. Acad. Sci. U.S.A. 64, 719–726
30 Shinitzky, M. and Barenholz, Y. (1974) J. Biol. Chem. 249, 2652–2657
31 Lowry, O.H., Rosebrough, N.J., Farr, A.L. and Randall, R.J. (1951) J. Biol. Chem. 193, 265–275
32 Bonsall, R.W. and Hunt, S. (1971) Biochim. Biophys. Acta 249, 281–284
33 Gordesky, S.E. and Marinetti, G.V. (1973) Biochem. Biophys. Res. Commun. 50, 1027–1031
34 Litman, B.J. (1973) Biochemistry 12, 2545–2554
35 Gordesky, S.E., Marinetti, G.V. and Love, R. (1975) J. Membrane Biol. 20, 111–132
36 Rothman, J.E. and Kennedy, E.P. (1977) J. Mol. Biol. 110, 603–618
37 Vale, M.G.P. (1977) Biochim. Biophys. Acta 479, 39–48
38 Fontaine, R.N. and Schroeder, F. (1979) Biochim. Biophys. Acta 558, 1–12
39 Wisnieski, B.J. and Iwata, K.K. (1977) Biochemistry 16, 1321–1326
40 Weber, G. (1952) Biochem. J. 51, 145–155
41 Bretscher, M.S. (1976) Nature 260, 21–22
42 Schroit, A.J. and Pagano, R.E. (1981) Cell 23, 105–112
43 Shinitzky, M., Dianoux, A.C., Gitler, C. and Weber, G. (1971) Biochemistry 10, 2106–2113
44 Hare, F., Amiell, J. and Lussan, C. (1979) Biochim. Biophys. Acta 555, 388
45 Van Blitterswijk, W.J., Van Hoeven, R.P. and Van der Meer, B.W. (1981) Biochim. Biophys. Acta 644, 323–332
46 Shinitzky, M. and Yuli, I. (1981) Chem. Phys. Lipids, in the press
47 Andrich, M.P. and Vanderkooi, J.M. (1976) Biochemistry 15, 1257–1261
48 Heyn, M.P., Cherry, R.J. and Dencher, N.A. (1981) Biochemistry 20, 840–849
49 Yuli, I., Willrandt, W. and Shinitzky, M. (1981) Biochemistry 20, 4250–4256